▮ Materials Science inc. Nanomaterials & Polymers

Scalable Synthesis of Micron Size Crystals of CH₃NH₃PbI₃ at Room Temperature in Acetonitrile via Rapid Reactive Crystallization

Taame A. Berhe,[a] Wei-Nien Su,*[a] Ju-Hsiang Cheng,[b] Ming-Hsien Lin,[b] Kassa B. Ibrahim,[a] Amaha W. Kahsay,[b] Chia Lin Li,[d] Alok M. Tripathi,[b] Mau-Tsu Tang,[c] and Bing-Joe Hwang*[b, c]

From application point of view, scalable, facile and rapid synthesis method for mass production of a homogeneous and phase pure CH₃NH₃PbI₃ micron size crystal at the industry level is still highly required, although it has been claimed that the CH₃NH₃PbI₃ crystals can be prepared by solution-annealing the precursors at elevated temperature or prolonged reaction time. Herein, polycrystalline CH₃NH₃PbI₃ micron size crystals can be prepared by reactive crystallization of PbI₂ and CH₃NH₃I in a stoichiometric ratio at room temperature. TXM (Transmission X-ray Microscopy), optical microscope, TEM and TEM-EDX analysis were used to confirm the nature of the CH₃NH₃PbI₃ product. Moreover, Ostwald ripening of iodide ion into PbI₂ is proposed as the key step to form 3D PbI₃⁻, followed by the intercalation of CH₃NH₃⁺ for this reactive crystallization. Interestingly, this result suggests that industry level mass production of micron CH₃NH₃PbI₃ crystals is possible with this novel synthesis method.

1. Introduction

Since their pioneering from 2009,[1] CH₃NH₃PbI₃ perovskite materials have fascinated substantial concentration owing to their potential application in economical power conversion photovoltaics. Solar cell device based on these materials has achieved power conversion efficiency of 22.1%,[2] making this the fastest-advancing solar technology to date.[3] This is recorded as nine-fold step-up in cell efficiency within seven years[4] and the device has theoretical maximum beyond the 30% efficiency record.[5] This astonishing performance has benefitted from material properties ideally well-matched to photovoltaics, including direct band gaps, long charge carrier diffusion lengths and low carrier effective masses, high absorption coefficients, defect tolerance, and compatibility with low-cost, solution-supported fabrication procedures,[6] and overcoming the conventional limitation of solution-processed semiconductors.[7]

Micro-structured and Nano-structured perovskites are of great interest because they can have chemical and physical properties that are neither characteristic of the bulk nor of the atoms counterparts. Due to its large ratio of surface area to volume can contribute to enhance the light scattering effect and light harvesting, and thus exhibit photodetection performance better than bulky counterparts. Moreover, Perovskite nanoparticles have attracted attention due to their easy synthesis for highly luminescent colloidal quantum dot materials which are highly demanding in the field of LED devices, photodetectors and solar cell fabrication. Additionally, with the miniaturization of electronic devices, it has become increasingly important to investigate the size effects on the properties in the micron range approaching the nanometer scale ($\geq 1\,\mu m$). To achieve this goal, powders with controlled stoichiometric and, a small and uniform particle size are required, from which micron- and nano-structured CH₃NH₃PbI₃ perovskite materials can be prepared.

Literature reports disclose that the CH₃NH₃PbI₃ product is created only after annealing the precursors at elevate temperatures or prolonged reaction time.[8] Recently, Shen et al. discovered special function of DMF and unique presence of DMF-induced intermediate phase during perovskite crystallization.[9] The precipitation of perovskites crystals has been significantly inhibited before heat treatment due to the presence of solvent in the DMF-induced precursor film. Black precipitate of CH₃NH₃PbI₃ has been synthesized by precipitation from precursor solution of Lead(II) acetate by increasing the temperature to 100°C and then cooling back to 40°C.[10]

[a] Dr. T. A. Berhe, Prof. W.-N. Su, Dr. K. B. Ibrahim
NanoElectrochemistry Laboratory, Graduate Institute of Applied Science and Technology, National Taiwan University of Science and Technology, Taipei 106, Taiwan
E-mail: wsu@mail.ntust.edu.tw

[b] Dr. J.-H. Cheng, Prof. M.-H. Lin, Dr. A. W. Kahsay, Dr. A. M. Tripathi, Prof. B.-J. Hwang
NanoElectrochemistry Laboratory, Department of Chemical Engineering, National Taiwan University of Science and Technology, Taipei 106, Taiwan
E-mail: bjh@mail.ntust.edu.tw

[c] Dr. M.-T. Tang, Prof. B.-J. Hwang
National Synchrotron Radiation Research Center, Hsin-Chu, 30076, Taiwan

[d] C. Lin Li
Department of Material Science and Engineering, National Taiwan University of Science and Technology, Taipei 106, Taiwan

💻 Supporting information for this article is available on the WWW under https://doi.org/10.1002/slct.201904025

Likewise, polycrystalline $CH_3NH_3PbI_3$ black precipitate, obtained by drop-casting from equimolar mixtures of CH_3NH_3I and PbI_2 in gamma-butyrolactone heated to $100\,°C$ on glass substrate was recovered from the glass substrate.[11] In the same way, precursor solution of $CH_3NH_3PbI_3$ in DMF was drop cast onto glass substrates and annealed at $100\,°C$ and then the perovskites powder was collected by scratched off the substrate.[12] The bulk sample of $CH_3NH_3PbI_3$ powder was also prepared by dissolving equimolar CH_3NH_3I and PbI_2 in DMF, followed by evaporation of the solvent.[13,14] Dang *et al.* have reported bulk crystal growth of $CH_3NH_3PbI_3$ in the temperature range of $65–40\,°C$ after several days.[15] However, these synthetic methods may have some drawbacks: (1) complexity and mechanical degradation during product recovery using scratching off the film; (2) impossible to scale up for industrial mass production using film scratching off; (3) material degradation during prolong reaction time and slow evaporation since perovskite is sensitive to ambient conditions in the laboratory.

Additionally, Nakita K. Noel *et. al* introduced a new, low-boiling point, low viscosity solvent system that enables rapid, room temperature crystallization of methylammonium lead triiodide perovskite films using acetonitrile solvent.[16] The author able to produce dense, pinhole free films with uniform coverage, high specularity, and enhanced optoelectronic properties. However, their thin film synthesis procedure is too complex to use it to produce pure powder $CH_3NH_3PbI_3$ at industry level. Hence, it is important to find another room-temperature and facile synthesis approach to overcome such concerns for mass production of these hybrid halide perovskite materials, whose phase purity and homogeneity are essential to the fabrication of light emitting diode, photodetectors and solar cell devices. In parallel with establishing suitable synthesis methods of this pure chemical substance, the chemistry of formation that is: formation mechanisms, intermolecular exchange and intercalation mechanisms in addition to nucleation and growth mechanisms in solution are essential phenomena and need clear understanding for further development. This could lead for further optimizing the performance and stability of organolead halide hybrid perovskite solar cells.[17]

In this article, a scalable, facile and reproducible stoichiometrically optimized synthetic route at room temperature using acetonitrile as a solvent for the reaction between PbI_2 and CH_3NH_3I is reported. Pure and homogeneous phase $CH_3NH_3PbI_3$ micron size crystals with an average grain size of $\geq 1\,\mu m$ was synthesized. This thermodynamically driven spontaneous process occurred via Ostwald ripening. This may be due to the larger particles of PbI_2, which are energetically more stable than smaller particles of CH_3NH_3I and act as a reaction site for the formation of such crystals. This approach is chemical reaction driven reactive crystallization method. This result suggested that the synthesis route is low cost, green and readily scalable for both laboratory and industrial mass production, which is the first demonstration to the best of our knowledge to use this easy, direct and reproducible procedure with high yield ($\geq$ 93%) of the product at room temperature and one atmospheric pressure. The second advantage is that acetonitrile is an easily volatile solvent and can be easily recovered and suitable to

prepare bigger crystals of $CH_3NH_3PbI_3$ during industrial mass production, during which the final product is free of residual solvent. The third one is that it is promising and well suited to synthesize $CH_3NH_3PbI_3$ micron crystal materials, which suffer from decomposition due to elevated synthesis temperatures and extended synthesis time. Hence, this procedure demonstrated a practical method of getting pure chemical substances in a suitable form for storing and packaging of $CH_3NH_3PbI_3$ perovskites materials.

2. Results and Discussion

$CH_3NH_3PbI_3$ perovskites are highly attractive light absorber material and have promising potential applications for many optoelectronic devices. From an application point of view, pure $CH_3NH_3PbI_3$ chemical substance is highly required. For this purpose, a facile, green and scalable synthesis method for both laboratory and industry scales was developed. Acetonitrile was used as solvent media for this suitable approach for producing, storing and packaging of $CH_3NH_3PbI_3$ pure chemical substance. After mixing both PbI_2 and CH_3NH_3I reactants in acetonitrile, black crystals of $CH_3NH_3PbI_3$ formed immediately at room temperature and the solution was stirred for 5 min to obtain a homogenous mixture of the $CH_3NH_3PbI_3$ crystals as shown in Scheme 1. The solvent was filtered using Whatman filter paper. Then, the product was washed again using acetonitrile to remove the unreacted excess reactants remaining in the solution. Finally, the product was dried in an oven at $60\,°C$ for not greater than 60 minutes to remove the residual solvent and $\geq 93\%$ yield of $CH_3NH_3PbI_3$ was recovered.

Thus, the advantages of the new method are: a) no side product, b) fast reaction, c) reaction at room temperature and mild conditions, d) color change that provides a visual means for ascertaining the progress of the reaction and suitable to prepare bigger single and powder crystals of $CH_3NH_3PbI_3$. Furthermore, we tested other solvents such as DMF, DMSO, γ-butyrolactone, acrylonitrile and alcohols for this purpose, but it was not successful except acrylonitrile (Sigma Aldrich, $\geq 98\%$). Hence, we successfully synthesized $CH_3NH_3PbI_3$ micron size crystals at room temperature and our procedure demonstrated a practical method of getting pure chemical substances in a suitable form for storing and packaging of $CH_3NH_3PbI_3$ perovskites materials as summarized in Figure 1A and Figure 1B. This indicated that the micron size crystals observed by the micrometer level optical microscope was well supported by
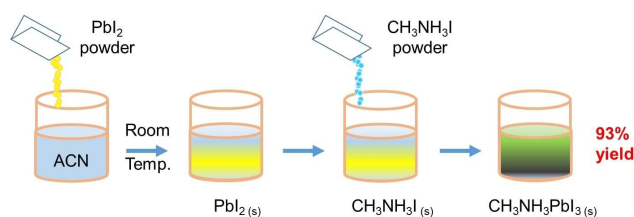
Scheme 1. Synthesis procedure of $CH_3NH_3PbI_3$ crystals via stoichiometrically optimized reactive crystallization.
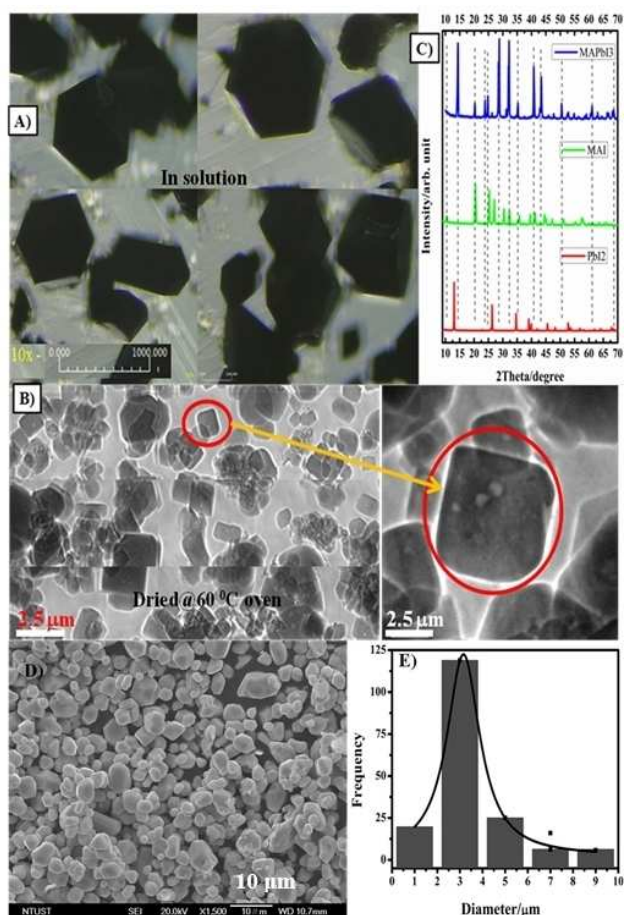
Figure 1. Image of micron size CH₃NH₃PbI₃ crystals captured: using optical microscope in solution (A), Transmission X ray Microscopy (B) after oven dried at 60 °C, the obtained diffraction patterns (C) and its Scanning Electron Microscope (SEM) image (D) with statistics of the crystal sizes (E).

FTO. To further confirm the morphology of the micron size crystals and its size distribution, we carried out scanning electron microscope as shown in Figure 1D. The average size distribution of the micron size perovskite crystals is 3.16 ± 0.89 µm. The frequency of the crystal size distributed in the range of 2 µm to 4 µm is highest in perovskite recorded in this study. Crystal growth at/or nearer to ambient temperature reduces the possibility of major thermal shock to the crystal both during growth and removal from the apparatus. Growth of crystals from solution at room temperature has many advantages over other growth methods though the rate of crystallization is slow. Since growth is carried out at room temperature, the structural imperfections in solution grown crystals are relatively low.[20]

The nature of the synthesized micron size crystals in Acetonitrile using TEM: The bright field (Figure 2a) and high magnitude TEM (Figure 2b) as well as the selected area electron diffraction pattern (SAED) analysis (Figure 2c) were used to characterize CH₃NH₃PbI₃ powder. The SAED pattern with the appearance of the rings, which indicates the synthesized CH₃NH₃PbI₃ micron size crystals is fully crystalline with poly-crystalline nature. Moreover, the high resolution TEM image (Figures 2d&2e) showed high crystallinity of CH₃NH₃PbI₃ nano-particles with polycrystalline nature and the appearance of lattice fringes. The high resolution TEM image confirms dis*tinct*

the transmission X ray microscopy (TXM), which has the highest optical resolution better than 30 nm in 2D (third order), better than 60 nm (first order) and close to 60 nm in 3D. It also equipped with phase contrast with both Zernike's phase contrast and propagation based. This is the first TXM to use the capillary as the condenser, and this design gives one order magnitude higher than the traditional type, which use zoneplate as condenser.[18] Furthermore, as shown in Figure 1C, the synchrotron XRD intensities are located at 2Theta value of 14.08, 19.91, 23.45, 24.47, 28.15, 28.43, 30.88, 31.63, 31.84, 34.95, 40.44, 40.63, 45.70, 47.40 and 50.20°. Furthermore, all these intensities correspond to the (110), (112), (211), (202), (004), (220), (213), (310), (114), (312), (224), (411), (332), (206) and (404) planes, respectively, which confirmed the crystal structure of this micron sized crystals of CH₃NH₃PbI₃ is tetragonal symmetry at room temperature.[11,15] Many literature did not report the Synchrotron based XRD(SXRD) peaks located at 23.45 and 24.47° assigned to (211) and (202) due to overlapping with FTO peaks or dominated by the nearby FTO peaks.[7b,19] These two SXRD peaks appeared mainly due to the formation of CH₃NH₃PbI₃ micron size crystals, but not due to
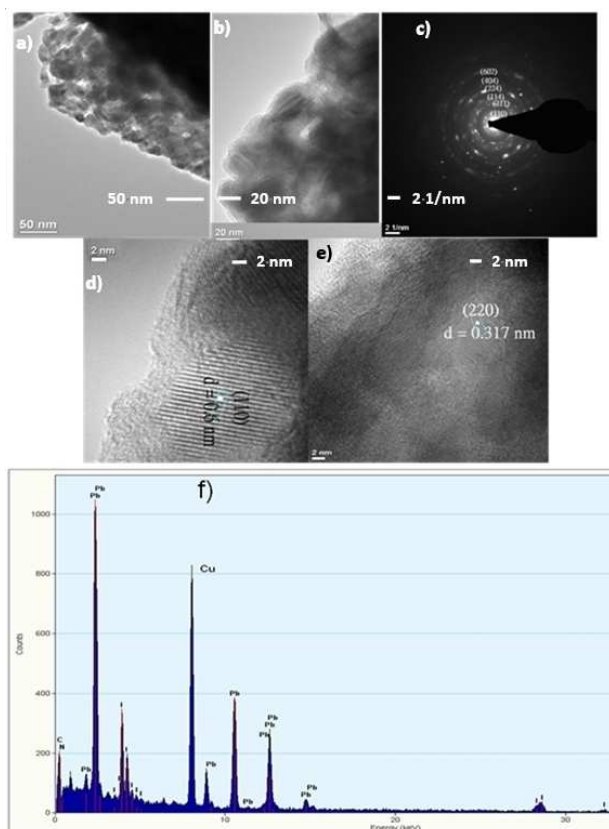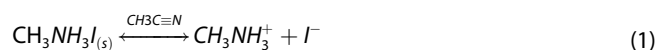

Figure 2. Bright field TEM (a) and high-magnitude TEM image (b), SAED (c), HRTEM image of the surface structure at the edge (d) and (e) for CH₃NH₃PbI₃ powder, and TEM-EDX analysis elemental analysis (f).

lattice spacing. The distance between the two lattice fringes is 6.01 Å and 3.15 Å, which correspond to the (110) and (220) plane of the $CH_3NH_3PbI_3$ crystal, respectively. This confirmed the proper phase formation of the $CH_3NH_3PbI_3$ material. In most literatures (110) facet has been widely reported as the main plane indicating formation of tetragonal shape crystals. From our HRTEM result shown in Figure 2d, the d spacing is quite large for this facet *i.e.* 6 Å. This value indicates that the distribution of the atoms in the crystal plane is broad. This broad distribution of atoms indicates that the surface to volume (S/V) ratio of the crystals is larger. This larger S/V ratio of perovskites crystals reflects more reactive behavior of the surface of perovskites materials towards incoming atoms or molecules such as water molecules from the environment. The already known instability problems of perovskites materials towards the environment are believed to originate from the reactive moisture sensitive surface properties.[17] The other property is weak binding energy of $CH_3NH_3PbI_3$, *i.e.* less than 50 meV,[21] and promotes weakly bound 3D framework which is easily prone to environment, though this framework has excellent optoelectronic properties. The binding energy of a 2D system is four times larger than that of the corresponding 3D system.[22] Thus, as the semiconductor's dimensionality is increased, and then the excitonic binding energy as well as oscillator strength is reduced dramatically. Similarly, $CH_3NH_3PbBr_3$ has 3D framework but short ionic radius and larger binding energy due to bromine,[21] which make it better resistant towards environment compared to $CH_3NH_3PbI_3$. Atoms are loosely bound each other, broadly arranged and forming 3D framework, which has longer interconnection distance of atoms in $CH_3NH_3PbI_3$. The reason for weak binding energy of the 3D $CH_3NH_3PbI_3$ is small on-site coulomb energy.[23]
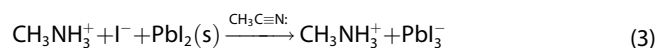
In order to understand the elemental composition of the synthesized micron size crystals, TEM-EDX analysis was carried out in a randomly selected area, as shown in Figure 2f. In the concentration profiles, Pb, I, C and N were detected. Moreover, along the selected area, one can claim that there are pristine $CH_3NH_3PbI_3$ nano-crystals. It is noteworthy to mention that the observed elemental analysis of pristine $CH_3NH_3PbI_3$ in Figure 2f are covered in a Cu grid; and due to the high Cu crystallinity, the Cu could able to be observed. Due to its heavy mass Pb gets strong intensity and followed by iodine. In other words, this analysis indicates that Pb and I have a wide distribution compared to the other light elements. Due to its high amount of surface, Pb gets stronger intensified and followed by iodine EDX.

The questions here are proposed to show how the crystals of $CH_3NH_3PbI_3$ form in the solution at room temperature when using acetonitrile as solvent. Larger particles of PbI_2 are more energetically more stable than smaller particles of CH_3NH_3I. Considering the high solubility of CH_3NH_3I and insoluble PbI_2 crystal in acetonitrile, PbI_2 crystal act as nuclei and attract I^- and $CH_3NH_3^+$ ions to its surface, respectively, from the solution. This is thermodynamically-driven spontaneous process occurring via Ostwald ripening of iodide ions into PbI_2 forming PbI_3^- and followed by intercalation of $CH_3NH_3^+$ cation into PbI_3^- forming 3D $CH_3NH_3PbI_3$. The overall reaction mechanism in the
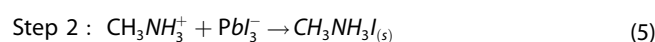
solution forming crystals of $CH_3NH_3PbI_3$ is proposed as equations 1-6 and presented in Scheme 2:

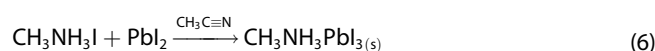$$CH_3NH_3I_{(s)} \xrightleftharpoons{CH3C\equiv N} CH_3NH_3^+ + I^- \tag{1}$$

$$PbI_2(s) \xrightarrow{CH_3C\equiv N} \text{no reaction} \tag{2}$$

Thus,

$$CH_3NH_3^+ + I^- + PbI_2(s) \xrightarrow{CH_3C\equiv N:} CH_3NH_3^+ + PbI_3^- \tag{3}$$

From Equation (3) it can be proposed that:

$$\text{Step 1}: \ I^- + PbI_2 \rightarrow PbI_3^- \tag{4}$$

$$\text{Step 2}: \ CH_3NH_3^+ + PbI_3^- \rightarrow CH_3NH_3I_{(s)} \tag{5}$$

Therefore,

$$CH_3NH_3I + PbI_2 \xrightarrow{CH_3C\equiv N} CH_3NH_3PbI_{3(s)} \tag{6}$$

Thus, the nature of the reaction and the formation of perovskites crystal in acetonitrile is spontaneous reaction. The role of the acetonitrile is dissolving the methylammonium iodide crystals and facilitates Ostwald ripening of iodide ion to form PbI_3^- octahedron with 3D framework followed by the intercalation of the $CH_3NH_3^+$, forming crystals of $CH_3NH_3PbI_3$ immediately. Thus, the Ostwald ripening of iodide ion into PbI_2 triggers the transformation of 2D PbI_2 into 3D PbI_3^- octahedral shape. Then counter cation $CH_3NH_3^+$ diffuse in into the center of PbI_3^- octahedron because of its small size forming inorganic-organic perovskites family of materials ABX_3 (A$=CH_3NH_3^+$; B$=Pb^{2+}$; and X$=I^-$ and/or other halide ions), which consists of the 3D network of $[PbI_6]^{4-}$ clusters. Here, each of $[PbI_6]^{4-}$ clusters are connected with six neighbors at the iodine ions, forming a 3D network of $[PbI_6]^{4-}$ octahedral. Finally, the formed black and highly crystalline crystals of $CH_3NH_3PbI_3$ will be precipitated. Thus, acetonitrile was added to cause a chemical reaction to occur by promoting the (1) formation of both $CH_3NH_3^+$ and I^- ions in the solution; (2) facilitating Ostwald ripening of I^- ions and intercalation of $CH_3NH_3^+$ into $[PbI_3]^-$ octahedral and (3) facilitating rearrangement of 2D $[PbI_6]^{4-}$ network of atoms into 3D $[PbI_6]^{4-}$ network.

In summary, the proposed mechanism in Scheme 2 verified that 1) acetonitrile dissolved CH_3NH_3I into iodide anion and $CH_3NH_3^+$ cation; 2) these ions diffuse simultaneously into the surface of PbI_2 crystals and reaction start on the surface of PbI_2 to form PbI_3^- by iodide Ostwald ripening and then perovskites on surface; 3) then gradually the reaction completed and all PbI_2 become reacted with iodide ion by Ostwald ripening forming PbI_3^- clusters and quick intercalation of $CH_3NH_3^+$ take place forming the final product $CH_3NH_3PbI_3$. Thus kinetically the first reaction is expected to be Ostwald ripening of iodide anion and then intercalation of the organic cation. By this reactive crystallization method larger crystals of perovskites can be synthesized.
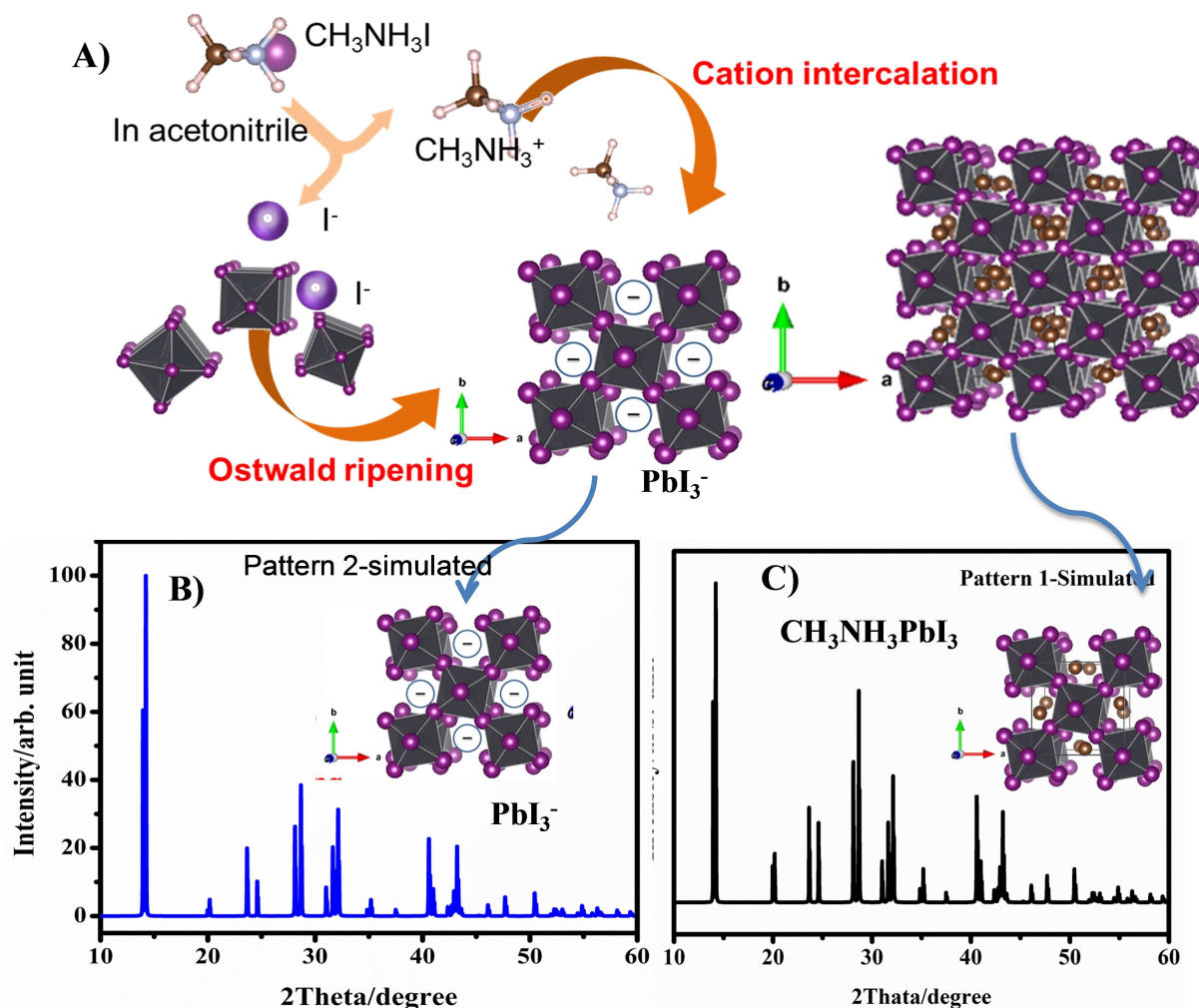
Scheme 2. (A) Proposed micron size crystal formation mechanism of $CH_3NH_3PbI_3$ in acetonitrile at room temperature with Ostwald ripening and intercalation of ions. (B) (C) Simulated XRD patterns of tetragonal $CH_3NH_3PbI_3$ at 25 °C with different structural arrangements during different crystal growth stages.

3. Conclusion

Although $CH_3NH_3PbI_3$ is a promising light harvesting material that has attracted significant interest in recent years, the synthesis of its single crystal and micron size crystals becomes challenging due to its sensitivity towards the environmental factors. Unexpectedly, it was possible to synthesize pure phase of $CH_3NH_3PbI_3$ micron size crystals of ≥ 1 μm, with an average size distribution of 3.155 ± 0.889 μm and high reproducible yield of $\geq 93\%$ at room temperature using 0.693 g: 0.239 g stoichiometric ratio of PbI_2:CH_3NH_3I by reactive crystallization approach in ACN. The role of acetonitrile is promoting the (1) formation of both I^- and $CH_3NH_3^+$ ions in the solution; (2) facilitating Ostwald ripening of I^- ion and intercalation of $CH_3NH_3^+$ cation into $[PbI_6]^{4-}$ octahedral, respectively, and (3) facilitating rearrangement of 2D $[PbI_6]^{4-}$ network of atoms into 3D $[PbI_6]^{4-}$ network. The insoluble crystals of PbI_2 act as nuclei for the formation of $CH_3NH_3PbI_3$ powder in ACN. In addition, an excellent solubility of CH_3NH_3I in ACN could be responsible for the efficient intercalation process of $CH_3NH_3^+$ cations into the lead halide crystal frameworks, resulting in the formation of compact and homogeneous crystal nuclei. The initial PbI_6 octahedral crystals could be rearranged in the ionic liquid systems by Ostwald ripening during thermal annealing in order to reduce the surface energy and form thermodynamically more stable perovskites structures. This reactive crystallization method is expected to be suitable for mass production of larger crystals of perovskites at industry level.

Supporting Information Summary

The supporting information includes the synthesis and characterization of $CH_3NH_3PbI_3$ micron size crystals as well as testing conditions during characterizations.

[1] A. Kojima, K. Teshima, Y. Shirai, T. Miyasaka, *J. Am. Chem. Soc.* **2009**, *131*, 6050–6051.

[2] W. S. Yang, B.-W. Park, E. H. Jung, N. J. Jeon, Y. C. Kim, D. U. Lee, S. S. Shin, J. Seo, E. K. Kim, J. H. Noh, S. I. Seok, *Science* **2017**, *356*, 1376–1379.

[3] S. Collavini, S. F. Völker, J. L. Delgado, *Angew. Chem. Int. Ed. Engl.* **2015**, *54*, 9757–9759.

[4] H. Zhou, Q. Chen, G. Li, S. Luo, T.-B. Song, H.-S. Duan, Z. Hong, J. You, Y. Liu, Y. Yang, *Science* **2014**, *345*, 542–546.

[5] C. D. Bailie, M. G. Christoforo, J. P. Mailoa, A. R. Bowring, E. L. Unger, W. H. Nguyen, J. Burschka, N. Pellet, J. Z. Lee, M. Gratzel, R. Noufi, T. Buonassisi, A. Salleo, M. D. McGehee, *Energy Environ. Sci.* **2015**, *8*, 956–963.

[6] a) C. C. Stoumpos, C. D. Malliakas, M. G. Kanatzidis, *Inorg. Chem.* **2013**, *52*, 9019-9038; b) C. S. Ponseca, T. J. Savenije, M. Abdellah, K. Zheng, A. Yartsev, T. Pascher, T. Harlang, P. Chabera, T. Pullerits, A. Stepanov, J.-P. Wolf, V. Sundström, *J. Am. Chem. Soc.* **2014**, *136*, 5189-5192; c) G. Xing, N. Mathews, S. Sun, S. S. Lim, Y. M. Lam, M. Grätzel, S. Mhaisalkar, T. C. Sum, *Science* **2013**, *342*, 344-347; d) L. Etgar, P. Gao, Z. Xue, Q. Peng, A. K. Chandiran, B. Liu, M. K. Nazeeruddin, M. Grätzel, *J. Am. Chem. Soc.* **2012**, *134*, 17396–17399.

[7] a) J. M. Ball, M. M. Lee, A. Hey, H. J. Snaith, *Energy Environ. Sci.* **2013**, *6*, 1739-1743; b) N. J. Jeon, J. H. Noh, Y. C. Kim, W. S. Yang, S. Ryu, S. I. Seok, *Nat. Mater.* **2014**, *13*, 897-903; c) J. Burschka, N. Pellet, S.-J. Moon, R. Humphry-Baker, P. Gao, M. K. Nazeeruddin, M. Gratzel, *Nature* **2013**, *499*, 316-319; d) D. Liu, T. L. Kelly, *Nat. Photonics* **2014**, *8*, 133-138; e) G. E. Eperon, S. D. Stranks, C. Menelaou, M. B. Johnston, L. M. Herz, H. J. Snaith, *Energy Environ. Sci.* **2014**, *7*, 982-988; f) G. Hodes, *Science* **2013**, *342*, 317–318.

[8] A. Dualeh, N. Tétreault, T. Moehl, P. Gao, M. K. Nazeeruddin, M. Grätzel, *Adv. Funct. Mater.* **2014**, *24*, 3250–3258.

[9] D. Shen, X. Yu, X. Cai, M. Peng, Y. Ma, X. Su, L. Xiao, D. Zou, *J. Mater. Chem. A* **2014**, *2*, 20454–20461.

[10] A. Poglitsch, D. Weber, *J. Chem. Phys.* **1987**, *87*, 6373–6378.

[11] T. Baikie, Y. Fang, J. M. Kadro, M. Schreyer, F. Wei, S. G. Mhaisalkar, M. Graetzel, T. J. White, *J. Mater. Chem. A* **2013**, *1*, 5628–5641.

[12] A. Dualeh, P. Gao, S. I. Seok, M. K. Nazeeruddin, M. Grätzel, *Chem. Mater.* **2014**, *26*, 6160–6164.

[13] J. Yang, B. D. Siempelkamp, D. Liu, T. L. Kelly, *ACS Nano* **2015**, *9*, 1955–1963.

[14] J. Xie, Y. Liu, J. Liu, L. Lei, Q. Gao, J. Li, S. Yang, *J. Power Sources* **2015**, *285*, 349–353.

[15] Y. Dang, Y. Liu, Y. Sun, D. Yuan, X. Liu, W. Lu, G. Liu, H. Xia, X. Tao, *CrystEngComm* **2015**, *17*, 665–670.

[16] N. K. Noel, S. N. Habisreutinger, B. Wenger, M. T. Klug, M. T. Hörantner, M. B. Johnston, R. J. Nicholas, D. T. Moore, H. J. Snaith, *Energy Environ. Sci.* **2017**, *10*, 145–152.

[17] T. A. Berhe, W.-N. Su, C.-H. Chen, C.-J. Pan, J.-H. Cheng, H.-M. Chen, M.-C. Tsai, L.-Y. Chen, A. A. Dubale, B.-J. Hwang, *Energy Environ. Sci.* **2016**, *9*, 323-356.

[18] http://tpsbl.nsrrc.org.tw/bd_page.aspx?lang=en&port=31 A&pid=1138, 31AProjection x-ray microscope and Transmission x-ray microscope.

[19] X. Gao, J. Li, J. Baker, Y. Hou, D. Guan, J. Chen, C. Yuan, *Chem. Commun. (Camb.)* **2014**, *50*, 6368–6371.

[20] J. C. Brice, *The growth of crystal from liquids,* Wiley, New York **1973**.

[21] K. Tanaka, T. Takahashi, T. Ban, T. Kondo, K. Uchida, N. Miura, *Solid State Commun.* **2003**, *127*, 619–623.

[22] G. C. Papavassiliou, *Prog. Solid State Chem.* **1997**, *25*, 125–270.

[23] M. Hirasawa, T. Ishihara, T. Goto, *J. Phys. Soc. Jpn.* **1994**, *63*, 3870–3879.